

Imitation learning for variable speed motion generation over multiple actions

Yuki Saigusa¹, Ayumu Sasagawa², Sho Sakaino³ and Toshiaki Tsuji⁴

Abstract—Robot motion generation methods using machine learning have been studied in recent years. Bilateral control-based imitation learning can imitate human motions using force information. By means of this method, variable speed motion generation that considers physical phenomena such as the inertial force and friction can be achieved. Previous research demonstrated that the complex relationship between the force and speed can be learned by using a neural network model. However, the previous study only focused on a simple reciprocating motion. To learn the complex relationship between the force and speed more accurately, it is necessary to learn multiple actions using many joints. In this paper, we propose a variable speed motion generation method for multiple motions. We considered four types of neural network models for the motion generation and determined the best model for multiple motions at variable speeds. Subsequently, we used the best model to evaluate the reproducibility of the task completion time for the input completion time command. The results revealed that the proposed method could change the task completion time according to the specified completion time command in multiple motions.

I. INTRODUCTION

In recent years, it has been increasingly expected that robots can flexibly adapt their movements to changes in the environment. To realize such flexible motions, numerous researchers have focused on motion generation methods using machine learning [1]–[3]. Methods based on machine learning can be divided into two approaches.

The first approach is based on reinforcement learning [4]. In this approach, robots learn autonomously through trial and error based on the rewards that are designed by humans. The method of Levine *et al.* succeeded in gripping various objects using reinforcement learning [5]. However, the search space for robots to acquire skills is extremely large. Therefore, this approach requires a large number of trials [6]. Moreover, it is difficult to design rewards. Although methods for automating the design of these rewards have been studied [7], a technique that can be adapted to general tasks has not yet been realized.

The second approach is known as imitation learning or learning from demonstration [8]–[10]. Imitation learning is

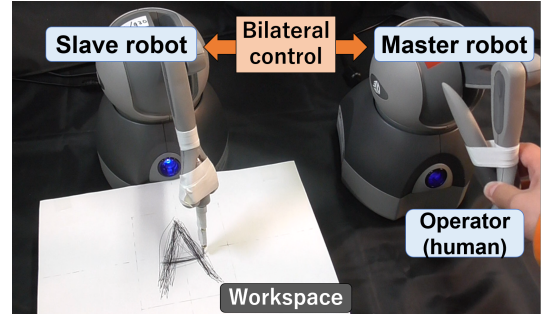


Fig. 1. Collection of training data using bilateral control

supervised learning from motion data that are demonstrated by humans. Therefore, the search space is appropriately restricted and it is not necessary to design rewards. Imitation learning using probabilistic models [11], neural networks (NNs) [12], [13], and dynamic movement primitives [14] have been proposed. Moreover, imitation learning using force information has been studied [15], [16]. A robot is more adaptable to environmental changes when using force information [17].

We previously proposed bilateral control-based imitation learning [18], [19]. Bilateral control is a teleoperation technique in which two robots are used: a master and a slave. Four-channel bilateral control synchronizes the position and presents the reaction force caused by the contact of the slave with the environment to the master [20]. Fig. 1 presents the collection of training data in bilateral control-based imitation learning. The operator operates the master robot and allows the slave robot to perform the task, at which time the motion data are saved. This approach can preserve human skills to compensate for control delays and dynamic robot interactions with the environment. The authors of [19] mentioned that this method enables the human equivalent speed of motion, which has not been possible in other imitation learning methods [10]–[17].

Generalization performance against operational speed is also studied in imitation learning. There is a method that can generate motion at multiple speeds [21]. However, the method in [21] cannot achieve the desired operating speed because the speed information is not input during learning. To execute the motion at the desired speed, it is necessary to consider the nonlinear relationship between the force and speed, taking into account factors such as friction and inertia. To achieve this, the speed and motion information need to be provided as inputs and their association should

¹Yuki Saigusa is with the Faculty of Engineering, Information and Systems, University of Tsukuba, Tsukuba 305-8577, Japan s2020741@s.tsukuba.ac.jp

²Ayumu Sasagawa was with the Department of Electrical and Electronic Systems Faculty of Engineering, Saitama University, Saitama 338-8570, Japan sasagawa.997@ms.saitama-u.ac.jp

³Sho Sakaino is with JST PRESTO and the Faculty of Engineering, Information and Systems, Department of Intelligent Interaction Technologies, University of Tsukuba, Tsukuba 305-8577, Japan sakaino@iit.tsukuba.ac.jp

⁴Toshiaki Tsuji is with the Department of Electrical and Electronic Systems Faculty of Engineering, Saitama University, Saitama 338-8570, Japan tsuji@ees.saitama-u.ac.jp

be learned. Taking advantage of our bilateral control-based imitation learning, we proposed a method that can generate variable speed motion [22]. In [22], the frequency command was input into the NN model. Thus, the NN model learned the physical phenomena relating to the motion speed and achieved variable speed operation in tasks that were greatly affected by friction and inertia. However, the work in [22] only considered reciprocating motion in which one axis moves significantly. Therefore, the basal movement was always constant, the movement space was small, and the posture almost did not change. That is, no significant change occurred in the spatial direction. The physical phenomena relating to the speed vary substantially depending on the robot posture, which has multiple degree of freedom (DOF) mechanisms. Therefore, it is necessary to learn various speeds for multiple actions that cause changes in the spatial direction. Furthermore, in [22], the motion speed was determined based on fast fourier transform. Thus, this method was limited to periodic motion.

In this paper, we propose a method that can generate variable speed motion for multiple actions. Because the proposed method inputs a task completion time as a command and the requirements for periodic motions are relaxed, it is applicable to most tasks. Furthermore, a structure that is suitable for variable speed operations for multiple actions is revealed. In this study, we first examined four different models with various input layers of the completion time and task commands. We also developed a model that can generate variable speeds for multiple actions. Thereafter, using the model, we examined the reproducibility of the task completion time for the input completion time commands. A letter writing task was conducted to verify the proposed method. According to the results, the proposed model can change the motion speed according to the input completion time command. The proposed model can generate slow motion by extrapolating the unlearned completion time command. The advantages of the proposed method are as follows:

- The NN model can learn the relationship between multiple actions and the speed.
- The NN model for learning the variable speed operation can be applied to most time-dependent tasks.

The remainder of this paper is organized as follows: Section II presents the robot control system and the bilateral control used in this study. In Section III, we describe bilateral control-based imitation learning and the proposed learning method. Section IV provides the experimental description, results, and discussion. Finally, in Section V, we conclude this study and discuss future research topics.

II. CONTROL SYSTEM

A. Manipulator

In this study, we used two TouchTM manipulators manufactured by 3D Systems, as illustrated in Fig. 2. This robot has three-DOFs and the angles θ_1 , θ_2 , and θ_3 corresponding to each joint are defined as per Fig. 2.

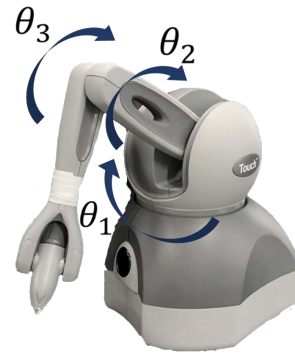


Fig. 2. Manipulator (TouchTM)

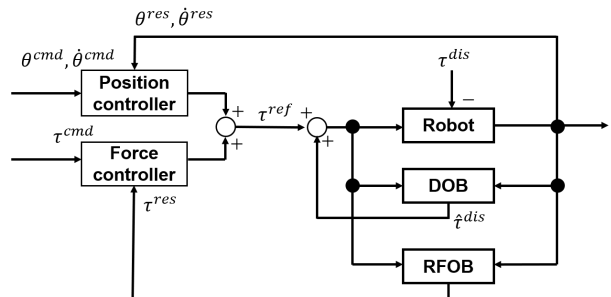


Fig. 3. Block diagram of manipulator controller

B. Controller

In this study, the manipulator control system consisted of a position controller and a force controller. The position controller consisted of a proportional and differential controller, whereas the force controller consisted of a proportional controller. The control system is depicted in Fig. 3. In the figure, θ , $\dot{\theta}$, and τ represent the joint angle, angular velocity, and torque, respectively, and the superscripts *cmd*, *res*, *ref*, and *dis* represent the command, response, reference, and disturbance values, respectively. The joint angle of each joint was obtained by the robot encoder and the angular velocity was calculated by its pseudo-differential. The disturbance torque τ^{dis} was calculated using a disturbance observer (DOB) [23] and the torque response value τ^{res} was calculated using a reaction force observer (RFOB) [24]. In this study, the dynamics model of the robot was assumed to be the same as that in [19]. The physical parameters were identified using the method described in [25].

C. Four-channel bilateral control

The bilateral control is described in this section. Four-channel bilateral control is a structure with a position controller and a force controller that are implemented on two robots: a master and a slave. This method is effective for imitation learning using force information [19]. Therefore, in this study, we used four-channel bilateral control. A block diagram of the four-channel bilateral control is presented in Fig. 4. The control goal of bilateral control is represented by

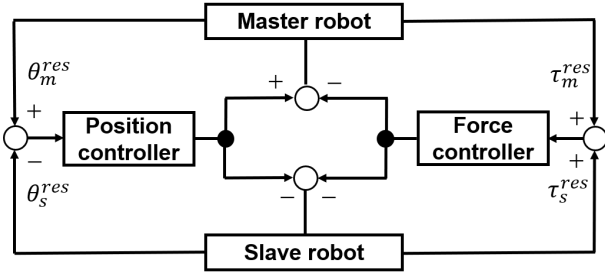


Fig. 4. Block diagram of four-channel bilateral control

the following equations:

$$\theta_m^{res} - \theta_s^{res} = 0, \quad (1)$$

$$\tau_m^{res} + \tau_s^{res} = 0, \quad (2)$$

where the subscript m represents the master and s represents the slave. Furthermore, θ_m^{res} , τ_m^{res} , θ_s^{res} , and τ_s^{res} are the master and slave variables, which are defined as follows:

$$\theta_m^{res} = \begin{bmatrix} \theta_{m1}^{res} \\ \theta_{m2}^{res} \\ \theta_{m3}^{res} \end{bmatrix}, \tau_m^{res} = \begin{bmatrix} \tau_{m1}^{res} \\ \tau_{m2}^{res} \\ \tau_{m3}^{res} \end{bmatrix}, \quad (3)$$

$$\theta_s^{res} = \begin{bmatrix} \theta_{s1}^{res} \\ \theta_{s2}^{res} \\ \theta_{s3}^{res} \end{bmatrix}, \tau_s^{res} = \begin{bmatrix} \tau_{s1}^{res} \\ \tau_{s2}^{res} \\ \tau_{s3}^{res} \end{bmatrix}, \quad (4)$$

The subscript numbers indicate the respective joints depicted in Fig. 2. Furthermore, the torque reference values for the bilateral control were calculated using the following equations:

$$\tau_m^{ref} = -\frac{J}{2}(K_p + K_d s)(\theta_m^{res} - \theta_s^{res}) - \frac{1}{2}K_f(\tau_m^{res} + \tau_s^{res}), \quad (5)$$

$$\tau_s^{ref} = \frac{J}{2}(K_p + K_d s)(\theta_m^{res} - \theta_s^{res}) - \frac{1}{2}K_f(\tau_m^{res} + \tau_s^{res}), \quad (6)$$

where K_p is the position control gain, K_d is the velocity control gain, K_f is the force control gain, J is the inertia, and s is the Laplace operator. The gains used in this study are listed in Table I.

III. METHOD

We used bilateral control-based imitation learning to generate variable speed motion for multiple actions. In this section, we explain the bilateral control-based imitation learning and describe the four types of NN models that were considered in this study.

A. Bilateral control-based imitation learning

1) *Collection of training data:* We experimented with the task of writing three letters ‘‘A,’’ ‘‘B,’’ and ‘‘C’’ at multiple speeds. In this section, we describe the collection of the training data for learning the behavior. The training data

TABLE I
GAIN OF ROBOT CONTROLLER

Parameter	Value	
K_p	Position feedback gain	121
K_d	Velocity feedback gain	22.0
K_f	Force feedback gain	1.00
g	Cut-off frequency of pseudo-derivative [rad/s]	40.0
g_{DOB}	Cut-off frequency of DOB [rad/s]	40.0
g_{RFOB}	Cut-off frequency of RFOB [rad/s]	40.0

were collected using two robots, as illustrated in Fig. 1. The operator controlled the master robot and executed the task by controlling the slave robot in the workspace. The joint angle, angular velocity, and torque of the master and slave robot data were saved at 1 kHz. The stroke orders of ‘‘A,’’ ‘‘B,’’ and ‘‘C’’ are depicted in Fig. 5. The training data were collected with a combination of the completion time and task commands, as indicated in the upper part of Table II. The training data were collected 10 times for each combination. Therefore, the number of training data collected was 90 (3[task commands] \times 3[completion time commands] \times 10[trials]). The collected 1 kHz data were downsampled to 50 Hz data for augmentation. The operator adjusted the task completion time by listening to a metronome. For each trial, the time from the start to the end of the task execution was saved as a label of the task execution time, and the label of the letter was also saved.

2) *Training the NN model:* An outline of the NN model used in this study is presented in Fig. 6. The NN model was configured to input the current response value of the slave robot, completion time command, and task command and to output the response value of the master robot after 20 ms. For the loss function, we used the mean squared error between the NN model output and teacher data. All input values were normalized using min-max normalization. The mini-batch consisted of 100 random sets.

3) *Autonomous operation:* The slave robot performed autonomous operation by using the learned model. During the autonomous operation, the current response values of the slave robot were measured in real time. These values were input into the NN model along with the completion time and task commands. Fig. 7 presents the difference between the system during the collection of the training data and during autonomous operation. The output values of the NN model were input into the slave controller as the next command value. This allowed the NN model to take the place of the master system and to reproduce the bilateral control.

B. Configuration of NN model

We conducted experiments using the NN models shown in Fig. 6. Conventionally, the NN model for learning variable speed motion has not been studied. In the field of multimodal learning, the discussion on how to fuse the information input into the NN model often arises [26]. Therefore, inputting all information into the input layer is not always the best means of training NN models. The model must be constructed based on this point. In this study, four types of NN models with

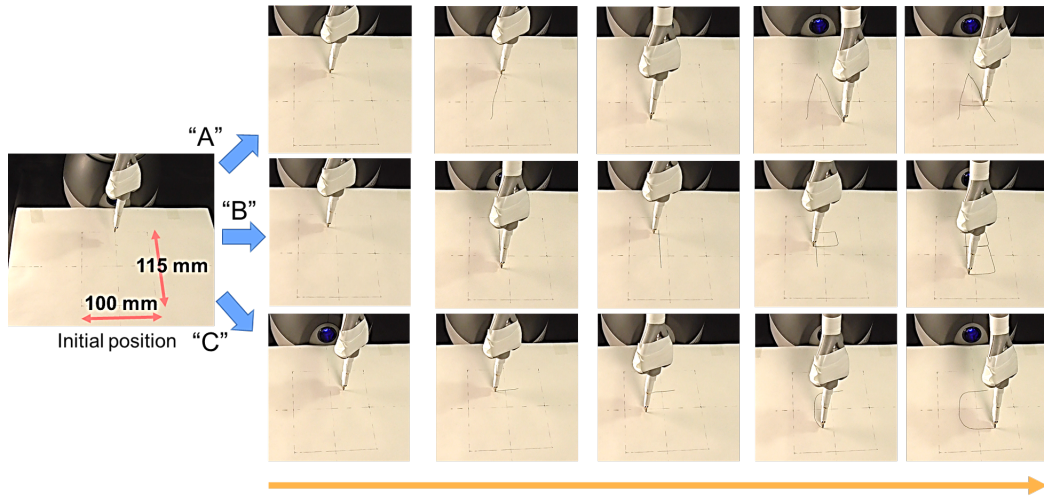


Fig. 5. Snapshot of task execution

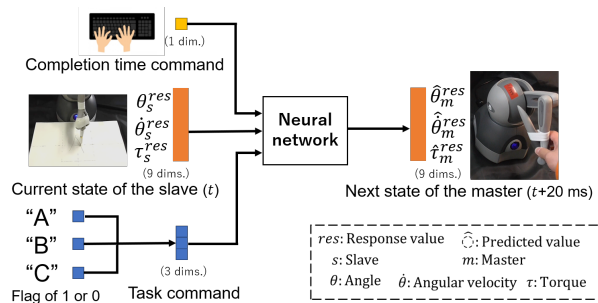


Fig. 6. Outline of NN model that learns multiple actions with variable speed

different ways of inputting the completion time and task commands were considered. The four models are presented in Fig. 8. All models were constructed with eight long short-term memory (LSTM) layers and a fully connected layer. The nodes in the middle layer were set to 50. The descriptions of the four models are as follows:

- SI-TI: All information is input into the input layer.
- SL-TL: The completion time command and task commands are input into the last LSTM layer.
- SI-TL: The completion time command is input into the input layer and the task command is input into the last LSTM layer.
- SL-TI: The task command is input into the input layer and the completion time command is input into the last LSTM layer.

IV. EXPERIMENT

We conducted preliminary experiments to determine the best NN model for generating multiple actions at variable speeds. Thereafter, further experiments were conducted to validate the effectiveness of the best NN model. This section describes the experiments and provides a detailed discussion of the results.

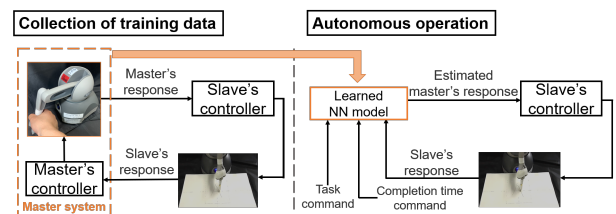


Fig. 7. Control system during data collection and autonomous operation. During autonomous operation, bilateral control is reproduced by the NN that takes the place of the human and the master robot.

A. Comparison of NN models

1) *Description:* A letter-writing task was performed using the four models described in Section III-B. The success of the task was defined as writing the letters in the same stroke order as in Fig. 5 without stopping. Furthermore, the letters should not exceed the frame shown in the initial position of Fig. 5, and humans should be able to recognize the letters. To succeed in this task, it is necessary to consider the complex relationship between the speed and force, as well as the relationships between movements. In particular, at low speeds, the frictional force becomes large and it is necessary to apply force to prevent the stroke from stopping. By comparing the success rates of the tasks, we determined the best model for generating variable speed movements for multiple actions. Each model was trained for 12,000 epochs using the training data described in Section III-A.2. In this experiment, evaluations were conducted for all combinations of the three task commands and the nine completion time commands illustrated in Table II. Five trials were conducted for each condition. Therefore, $135 (3[\text{task commands}] \times 9[\text{completion time commands}] \times 5[\text{trials}])$ trials were conducted using each model.

2) *Results:* The experimental results are displayed in Table III. SI-TL, in which the completion time command was entered in the input layer and the task command was entered in the last LSTM layer, exhibited the highest success

TABLE II

TRAINED/UNTRAINED COMPLETION TIME COMMANDS AND TASK COMMANDS USED IN EXPERIMENT

Task command	A						B						C					
Trained completion time command [s]	3.00	6.00	9.00				4.00	7.00	10.00				2.00	5.00	8.00			
Untrained completion time command [s]	2.00	4.00	5.00	7.00	8.00	10.00	2.00	3.00	5.00	6.00	8.00	9.00	3.00	4.00	6.00	7.00	9.00	10.00

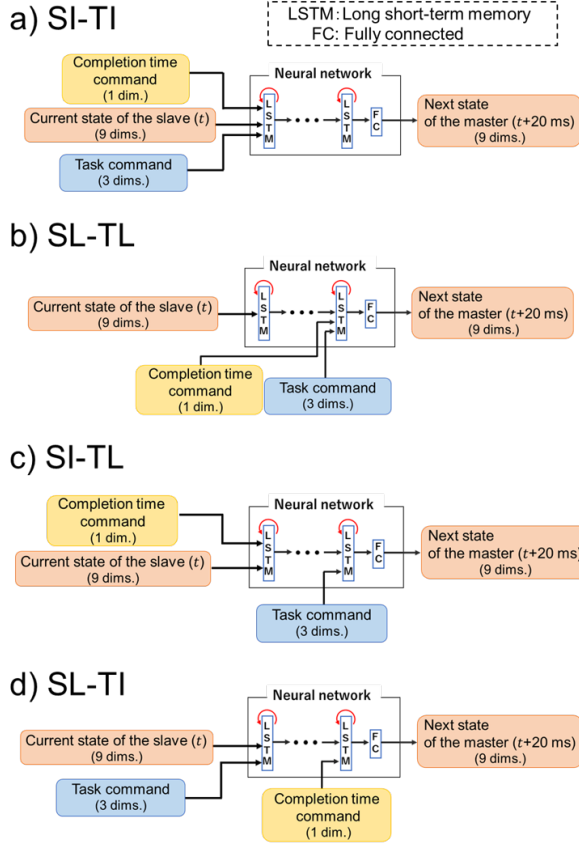


Fig. 8. Configuration of four models for verification.

rate. SI-TL could complete the task even when the unlearned combination of the completion time and task commands were input. The overall success rate of the other models was less than 30%. Therefore, SI-TL was the best model for learning the variable speed motion over multiple actions.

3) *Discussion:* For SL-TL and SL-TI, a longer completion time resulted in a lower success rate. In these models, the completion time command was not input into the input layer. Therefore, the relationship between the friction and motion speed could not be learned correctly and it was not possible to operate with an appropriate force against friction. In NNs, information with a high level of abstraction appears in the layer close to the inputs, and vice versa. Therefore, the task completion time, which is information with a high level of abstraction, should be provided in the input.

Many failures involved writing “B” and “C” confusedly, as shown in Fig. 9. In particular, the SI-TI model often failed. SI-TI input all of the information into the input layer. Because the task command was highly task-specific information, the low correlation between the layer close to the input and the task command would make the learning

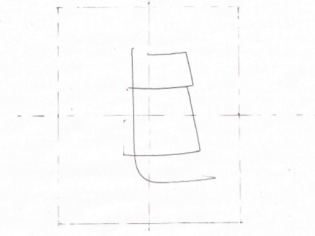


Fig. 9. Example of task failure

difficult. If the amount of training data increases in the future, the task success rate of SI-TI may be improved. However, it is desirable to be able to learn with a small amount of training data because the collection of training data is very costly. However, SI-TL can learn efficiently with less training data. In SI-TL, highly abstracted information; that is, the completion time command, was provided in the input, whereas task-specific information; that is, the task command, was provided close to the output. This structure matches the structure of NNs, which produce the highest level of abstraction at the input layer and task-oriented abstraction at the output layer. Thus, to learn variable speed motion generation for multiple motions efficiently, it is necessary to reflect the task commands after the appropriate extraction of the dynamic information.

B. Examination of task completion time repeatability for completion time command

1) *Description:* We investigated the reproducibility of the task completion time for the input completion time command of SI-TL. By comparing the input completion time command with the actual task completion time, we could examine whether SI-TL could learn the relationship between each action and speed.

2) *Results:* The experimental results are presented in Fig. 10. In this figure, only the successful completion of the task is plotted. There are few plot points for “B” because there were many failures. In Fig. 10, the black line represents the identity mapping. When the plots are along the line, this indicates that the reproducibility of the completion time is ideal. SI-TL could not perfectly reproduce the task completion time according to the completion time command. However, in most cases, the task was completed in a time close to the completion time command. As an additional experiment, three extrapolation completion times were tested. When the completion time command of 1.00 was input, the task could not be completed. However, when the 11.00 or 12.00 completion time commands were entered, the success rate of the task was 100%. Furthermore, for completion time commands of 11.00 and 12.00, SI-TL could slow down the

TABLE III
TASK EXECUTION RESULTS OF EACH MODEL

Model	Task Command	Success Rate[%]									Total
		Speed Command [sec]									
		2.00	3.00	4.00	5.00	6.00	7.00	8.00	9.00	10.00	
SI-TI	A	20(1/5)	20(1/5)	20(1/5)	0(0/5)	0(0/5)	0(0/5)	0(0/5)	0(0/5)	0(0/5)	16(21/135)
	B	0(0/5)	0(0/5)	0(0/5)	0(0/5)	0(0/5)	0(0/5)	0(0/5)	0(0/5)		
	C	80(4/5)	80(4/5)	100(5/5)	100(5/5)	0(0/5)	0(0/5)	0(0/5)	0(0/5)		
SL-TL	A	0(0/5)	100(5/5)	40(2/5)	0(0/5)	0(0/5)	0(0/5)	0(0/5)	0(0/5)	0(0/5)	24(32/135)
	B	0(0/5)	0(0/5)	0(0/5)	0(0/5)	0(0/5)	0(0/5)	0(0/5)	0(0/5)		
	C	100(5/5)	100(5/5)	100(5/5)	100(5/5)	100(5/5)	0(0/5)	0(0/5)	0(0/5)		
SI-TL	A	0(0/5)	100(5/5)	100(5/5)	100(5/5)	100(5/5)	0(0/5)	100(5/5)	100(5/5)	100(5/5)	74(100/135)
	B	0(0/5)	0(0/5)	100(5/5)	0(0/5)	0(0/5)	0(0/5)	100(5/5)	100(5/5)	100(5/5)	
	C	100(5/5)	100(5/5)	100(5/5)	100(5/5)	100(5/5)	100(5/5)	100(5/5)	100(5/5)		
SL-TI	A	40(2/5)	60(3/5)	100(5/5)	100(5/5)	40(2/5)	0(0/5)	0(0/5)	0(0/5)	0(0/5)	27(37/135)
	B	20(1/5)	60(3/5)	0(0/5)	0(0/5)	0(0/5)	0(0/5)	0(0/5)	0(0/5)		
	C	100(5/5)	100(5/5)	100(5/5)	20(1/5)	0(0/5)	0(0/5)	0(0/5)	0(0/5)		

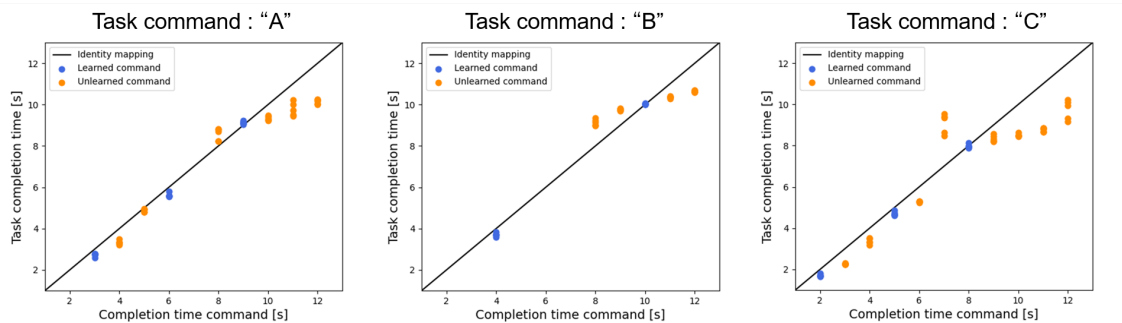


Fig. 10. Completion time command and actual task completion time

operation by inputting slower completion time commands. These experimental results indicate that the SI-TL model is capable of adapting variable speed motion generation to multiple motions, which was the goal of this study.

3) *Discussion*: The angular and torque response values during autonomous operation in the SI-TL model are depicted in Figs. 11 and 12. Owing to space limitations, the response values for task command “A” and the speed commands 3.00, 5.00, and 11.00 are shown. As indicated in the figure, SI-TL could change behavior in the time direction according to the completion time command. This behavior was not simply a linear expansion, but the force at each joint was appropriately modified according to the speed and relationship between each joint. SI-TL, which was the best model in this study, could complete the task without stopping, even if there was a large amount of friction owing to a low speed. By learning multiple motions relating to the speed, SI-TL could learn physical phenomena that were strongly related to the speed and posture through the robot body motion.

V. CONCLUSIONS

In this paper, we proposed a variable speed motion generation method for multiple actions. First, we considered models that learned the completion time and task commands. Among the four models examined, only SI-TL, which inputs the completion time command and robot response value into the input layer, and the task command into the final layer of the LSTM, could generate variable speed motions of multiple

actions with a high success rate. We also used this model to verify the reproducibility of the commands and found that it could reproduce unlearned speed commands appropriately.

It has recently been reported that the performance of a model can be improved by training multiple tasks in the field of self-supervised learning [27]. As the task completion time is an additional task that can be provided for almost any task and it can be treated as a subtask in self-supervised learning, self-supervised learning can be achieved in almost any task using the proposed framework. Note that self-supervised learning has conventionally been developed for spatial information, and temporal information has not been fully utilized. The proposed framework opens the possibility for self-supervised learning, which significantly contributes to understanding the dynamic phenomena in robotic tasks. In the future, we will examine the effectiveness of the proposed method in more detail by using a robot with multiple DOFs and a large mass to perform a task that is greatly affected by inertia. Subsequently, we will consider how the task can be executed more accurately within a specified task completion time.

ACKNOWLEDGMENT

This work was supported by the Japan Science and Technology Agency (JST) PRESTO, Grant Number JP-MJPR1755, Japan. This research was also supported by the Adaptable and Seamless Technology Transfer Program through Target-driven R&D (A-STEP) from the JST, Grant Number JPMJTR20RG.

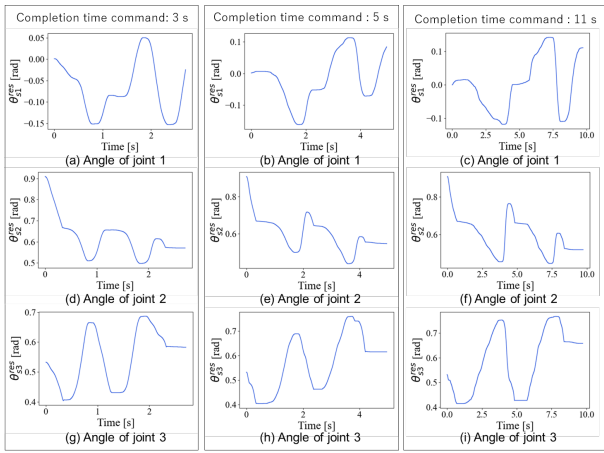


Fig. 11. Angle response values during autonomous operation

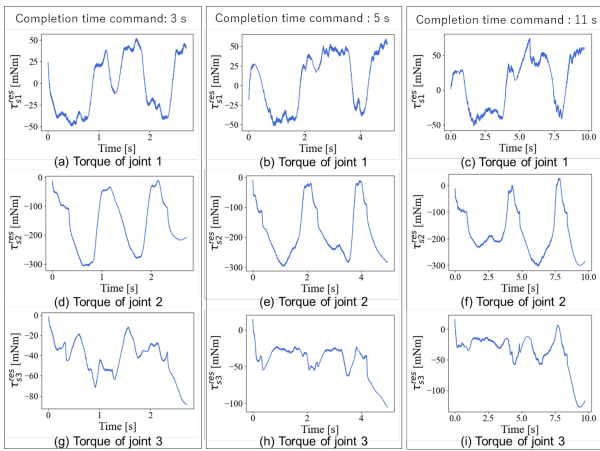


Fig. 12. Torque response values during autonomous operation

REFERENCES

- [1] S. Song, A. Zeng, J. Lee, and T. Funkhouser, “Grasping in the Wild: Learning 6DoF Closed-Loop Grasping from Low-Cost Demonstrations,” *IEEE Robotics and Automation Letters*, vol. 5, no. 3, pp. 4978–4985, 2020.
- [2] J. I. Lipton, A. J. Fay, and D. Rus, “Baxter’s Homunculus: Virtual Reality Spaces for Teleoperation in Manufacturing,” arXiv:1703.01270 [cs], 2017.
- [3] M. Kaspar, J. D. M. Osorio, and J. Bock, “Sim2Real Transfer for Reinforcement Learning without Dynamics Randomization,” in *Proceedings of the 2020 IEEE/RSJ International Conference on Intelligent Robots and Systems (IROS)*, pp. 4383–4388, 2020.
- [4] S. Levine, “Reinforcement Learning and Control as Probabilistic Inference: Tutorial and Review,” arXiv:1805.00909 [cs.LG], 2018.
- [5] S. Levine, P. Pastor, A. Krizhevsky, J. Ibarz, and D. Quillen, “Learning Hand-Eye Coordination for Robotic Grasping with Deep Learning and Large-Scale Data Collection,” *The International Journal of Robotics Research*, vol. 37, no. 4–5, pp. 421–436, 2017.
- [6] T. Tanaka, T. Kaneko, M. Sekine, V. Tangkaratt, and M. Sugiyama, “Simultaneous Planning for Item Picking and Placing by Deep Reinforcement Learning,” in *Proceedings of the 2020 IEEE/RSJ International Conference on Intelligent Robots and Systems (IROS)*, pp. 9705–9711, 2020.
- [7] G. Zuo, J. Lu, K. Chen, J. Yu, and X. Huang, “Accomplishing Robot Grasping Task Rapidly via Adversarial Training,” in *Proceedings of the 2019 IEEE International Conference on Real-time Computing and Robotics (RCAR)*, pp. 803–808, 2019.
- [8] H. Ravichandar, A. S. Polydoros, S. Chernova, and A. Billard, “Recent Advances in Robot Learning from Demonstration,” *Annual Review*

- of Control, Robotics, and Autonomous Systems*, vol. 3, pp. 297–330, 2020.
- [9] B. Fang, S. Jia, D. Guo, M. Xu, S. Wen, and F. Sun, “Survey of Imitation Learning for Robotic Manipulation,” arXiv:1703.09327 [cs.LG], 2017.
- [10] M. Laskey, J. Lee, R. Fox, A. Dragan, and K. Goldberg, “DART: Noise Injection for Robust Imitation Learning,” *Annual Review of Control, Robotics, and Autonomous Systems*, no. 3, pp. 362–369, 2019.
- [11] S. Calinon and A. Billard, “Incremental Learning of Gestures by Imitation in a Humanoid Robot,” in *Proceedings of the 2007 2nd ACM/IEEE International Conference on Human-Robot Interaction (HRI)*, pp. 255–262, 2007.
- [12] T. Zhang, Z. McCarthy, O. Jow, D. Lee, K. Goldberg, and P. Abbeel, “Deep Imitation Learning for Complex Manipulation Tasks from Virtual Reality Teleoperation,” arXiv:1710.04615v1, 2017.
- [13] P.-C. Yang, K. Sasaki, K. Suzuki, K. Kase, S. Sugano, and T. Ogata, “Repeatable Folding Task by Humanoid Robot Worker Using Deep Learning,” *IEEE Robotics and Automation Letters*, vol. 2, no. 2, pp. 397–403, 2016.
- [14] C. Yang, C. Zeng, C. Fang, W. He, and Z. Li, “A DMPs-Based Framework for Robot Learning and Generalization of Humanlike Variable Impedance Skills,” *IEEE/ASME Transactions on Mechatronics*, vol. 23, no. 3, pp. 1193–1203, 2018.
- [15] P. Kormushev, S. Calinon, and D. G. Caldwell, “Imitation Learning of Positional and Force Skills Demonstrated via Kinesthetic Teaching and Haptic Input,” *Advanced Robotics*, vol. 25, no. 5, pp. 581–603, 2011.
- [16] J. Silvério, Y. Huang, L. Rozo, S. Calinon, and D. G. Caldwell, “Probabilistic Learning of Torque Controllers from Kinematic and Force Constraints,” in *Proceedings of the 2020 IEEE/RSJ International Conference on Intelligent Robots and Systems (IROS)*, pp. 6552–6559, 2018.
- [17] A. X. Lee, H. Lu, A. Gupta, S. Levine, and P. Abbeel, “Learning Force-Based Manipulation of Deformable Objects from Multiple Demonstrations,” *2015 IEEE International Conference on Robotics and Automation (ICRA)*, pp. 177–184, 2015.
- [18] T. Adachi, K. Fujimoto, S. Sakaino, and T. Tsuji, “Imitation Learning for Object Manipulation Based on Position/Force Information Using Bilateral Control,” in *Proceedings of the 2018 IEEE/RSJ International Conference on Intelligent Robots and Systems (IROS)*, pp. 3648–3653, 2018.
- [19] A. Sasagawa, K. Fujimoto, S. Sakaino, and T. Tsuji, “Imitation Learning Based on Bilateral Control for Human-Robot Cooperation,” *IEEE Robotics and Automation Letters*, vol. 5, no. 4, pp. 6169–6176, 2020.
- [20] S. Sakaino, T. Sato, and K. Ohnishi, “Multi-DOF Micro-Macro Bilateral Controller Using Oblique Coordinate Control,” *IEEE Transactions on Industrial Informatics*, vol. 7, no. 3, pp. 446–454, 2011.
- [21] J. Tani and M. Ito, “Self-organization of Behavioral Primitives as Multiple Attractor Dynamics: A Robot Experiment,” *IEEE Transactions on Systems Man and Cybernetics, Part A*, vol. 33, no. 4, pp. 481–488, 2003.
- [22] S. Sakaino, K. Fujimoto, Y. Saigusa, and T. Tsuji, “Imitation Learning for Variable Speed Object Manipulation,” arXiv:2102.10283 [cs.RO], 2021.
- [23] K. Ohnishi, M. Shibata, and T. Murakami, “Motion Control for Advanced Mechatronics,” *IEEE/ASME Transactions on Mechatronics*, vol. 1, no. 1, pp. 56–67, 1996.
- [24] T. Murakami, F. Yu, and K. Ohnishi, “Torque Sensorless Control in Multidegree-of-Freedom Manipulator,” *IEEE Transactions on Industrial Informatics*, vol. 40, no. 2, pp. 259–265, 1993.
- [25] T. Yamazaki, S. Sakaino, and T. Tsuji, “Estimation and Kinetic Modeling of Human Arm using Wearable Robot Arm,” *IEEJ Transactions on Industry Applications*, vol. 199, no. 3, pp. 57–67, 2017.
- [26] K. Gadzicki, R. Khamsehashari, and C. Zetsche, “Early vs Late Fusion in Multimodal Convolutional Neural Networks,” in *Proceedings of the 2020 IEEE 23rd International Conference on Information Fusion (FUSION)*, pp. 1–6, 2020.
- [27] A. Jaiswal, A. R. Babu, M. Z. Zadeh, D. Banerjee, and F. Makedon, “A Survey on Contrastive Self-supervised Learning,” arXiv:2011.00362 [cs.CV], 2020.